Journal of Applied and Natural Science
17(3), 1345 - 1361 (2025)
ISSN : 0974-9411 (Print), 2231-5209 (Online)
journals.ansfoundation.org

Research Article

Modelling the spatial distribution of drought effects on land degradation in the Blue Nile Region, Sudan

Faroug A. Hassan*
Pan African University Life and Earth Sciences Institute (including Health and Agriculture), Ibadan, Nigeria; Land and Water Research Center, Land Evaluation Research Section, Agricultural Research Corporation (ARC), P.O. Box 126, Wad Medani, Sudan
Kolapo. O. Oluwasemire
Department of Soil Resources Management, Faculty of Agriculture, University of Ibadan, Ibadan, Nigeria
Abd Elmagid. A. Elmobarak
Soil Expert -ACSAD- Ministry of Environment, Water, and Agricultural (MEWA), Kingdom of Saudi Arabia (KSA)

*Corresponding author. E-mail: farougEH120@gmail.com

Article Info
https://doi.org/10.31018/jans.v17i3.6608
Received: February 06, 2025
Revised: August 27, 2025
Accepted: September 07, 2025

How to Cite
Hassan, F. A. *et al.* (2025). Modelling the spatial distribution of drought effects on land degradation in the Blue Nile Region, Sudan. *Journal of Applied and Natural Science*, 17(3), 1345 - 1361. https://doi.org/10.31018/jans.v17i3.6608

Abstract
Land degradation (LD) has a significant impact on Sudan's economy, society, and environment, driven by both climatic variations and human activities. Quantifying this degradation and its link to land use change (LUC) in Sudan's semiarid regions is crucial but often overlooked. The study provides precise spatiotemporal data to evaluate and model the impact of drought on land degradation in Sudan's Blue Nile Region. Four cloud-free Landsat images (1993, 2003, 2013, and 2023) were used and downloaded from the United States Geological Survey (USGS) repository. The study integrated vegetation indices (VIs) (NDVI, SARVI, SAVI, VHI) and soil indices (SIs) (BSI, TGSI) to assess LD. Change detection matrices estimated spatiotemporal land use and degradation shifts. Correlation and modeling (Kriging) determined relationships and causes of LD. Model validation was through the use of the coefficient of determination (R^2), , Kappa coefficient, and principal component analysis. SIs and VIs effectively detected LD. Very severe and severe degradation increased by 15.8% and 23.3%. Conversely, non and non-light-degraded areas decreased to 27% and 16.2%, respectively. Moderately degraded areas increased by 2.5% and 1.7%. The study revealed positive correlations between (TGSI, NDVI, VHI), with R^2 of 0.99, 0.98, respectively, and negative correlations between (BSI, NDVI, SAVI) with R^2 of -0.92 and -0.89. The Kriging model showed reasonable performance with an R^2 of 0.52, Kappa coefficients of 72%, and PC1 and PC2 capturing 78% of the variance. This work provides a robust, low-cost approach for predicting soil degradation via vegetation, especially valuable for semiarid regions. The integrated methodology and validation offer a reliable tool for environmental monitoring and management.

Keywords: Drought effect, land degradation, spatial distribution, sustainable land management, thematic mapper, vegetation indices

INTRODUCTION

Land degradation (LD) is a major global concern as it diminishes the planet's ability to provide food to the world (UNCCD, 2012; Chasek *et al*., 2019). Land degradation has become a significant concern in recent years, as it adversely affects hundreds of millions of people worldwide, leading to drought, famine, and the deterioration of soils and vegetation (Minelli *et al*., 2017). This issue is widely recognized as one of the most serious global environmental problems. According to Ekka *et al.* (2023), soil degradation, caused by natural and human-induced factors, poses a significant threat to global food security and ecosystem health. Drought, which is characterized by prolonged periods of insufficient rainfall, leads to reduced soil moisture, causing a series of negative effects on soil quality (Ejersa, 2021).

Climate variability worsens this degradation in regions vulnerable to drought, such as the Blue Nile Region of Sudan. Drought results in decreased soil moisture, increased erosion, and nutrient loss, ultimately reducing the land's agricultural productivity and ecological resilience (Webb *et al*., 2017). This is an urgent issue in

Sudan, where agriculture is a vital economic sector and rural communities heavily rely on the land for their livelihoods (Ali *et al*., 2020). Alredaisy (2023), highlighted the devastating impact of land degradation on large areas in Sudan, affecting social, economic, and environmental aspects. The Blue Nile Region is particularly vulnerable to drought impacts due to its semiarid climate and reliance on rain-fed agriculture (Mohamed, 2022). Many studies have shown that drought events in the region have become more frequent and intense because of climate change, leading to widespread soil degradation (Naumann et al., 2018; Grillakis 2019; and Hermans et al., 2021). However, these effects vary across the landscape (Yadeta *et al*., 2020).

Drought-induced soil degradation occurs through several mechanisms, including loss of vegetation cover and organic matter, increased soil erosion, salinization, and compaction; all of which reduce soil productivity (Zhang *et al*., 2019). Understanding the spatial distribution of these effects is crucial for implementing targeted land management strategies and mitigating degradation in vulnerable areas (Dieng *et al*., 2023). This highlights the need for a spatially explicit approach to assess and model the distribution of drought-induced soil degradation.

Merabti *et al*. (2023) and other researchers have used spatial modelling tools, including GIS and remote sensing, to capture and analyse the spatial variability of drought effects. By integrating environmental factors such as precipitation, vegetation indices, and soil properties, spatial models such as Kriging model can predict areas most vulnerable to soil degradation (Nzuza *et al*., 2021). These models provide valuable insights for land managers and policymakers to prioritize interventions, conserve soil resources, and mitigate the long-term impacts of drought on agricultural productivity and ecosystem services (Wang *et al*., 2023).

This research examines the impact of drought on soil degradation by incorporating multiple environmental covariates, laying the groundwork for targeted soil conservation strategies and sustainable land management practices. The other objective of this study was to model the spatial distribution of drought effects on soil degradation in the Blue Nile Region of Sudan and identify areas most at risk of degradation.

MATERIALS AND METHODS

Study area

The Blue Nile region is situated in southeastern Sudan, within the area of latitude 12.597386° to 9.490852°N and longitude 34.480218° to 33.951571°E and covers about 38,150.4 Km^2 (Fig 1). This region is characterized by calcitic and dolomitic marble meta-quartzites, crystalline schists, and gneisses, as mapped by Kabesh (1961). The metamorphism in the area has reached the amphibolite grade (Elzien *et al*., 2017), and these rocks have been identified as the oldest in the region. The geological formation is covered with substantial alluvial/colluvial deposits, with a clayey bottom layer and river sediments on top. The mean annual temperature is 27.6 °C (Taye *et al*., 2015), with a mean maximum of about 46.8 °C in April and a mean minimum of about 21.0 °C in January. Elnashi and Ahamed

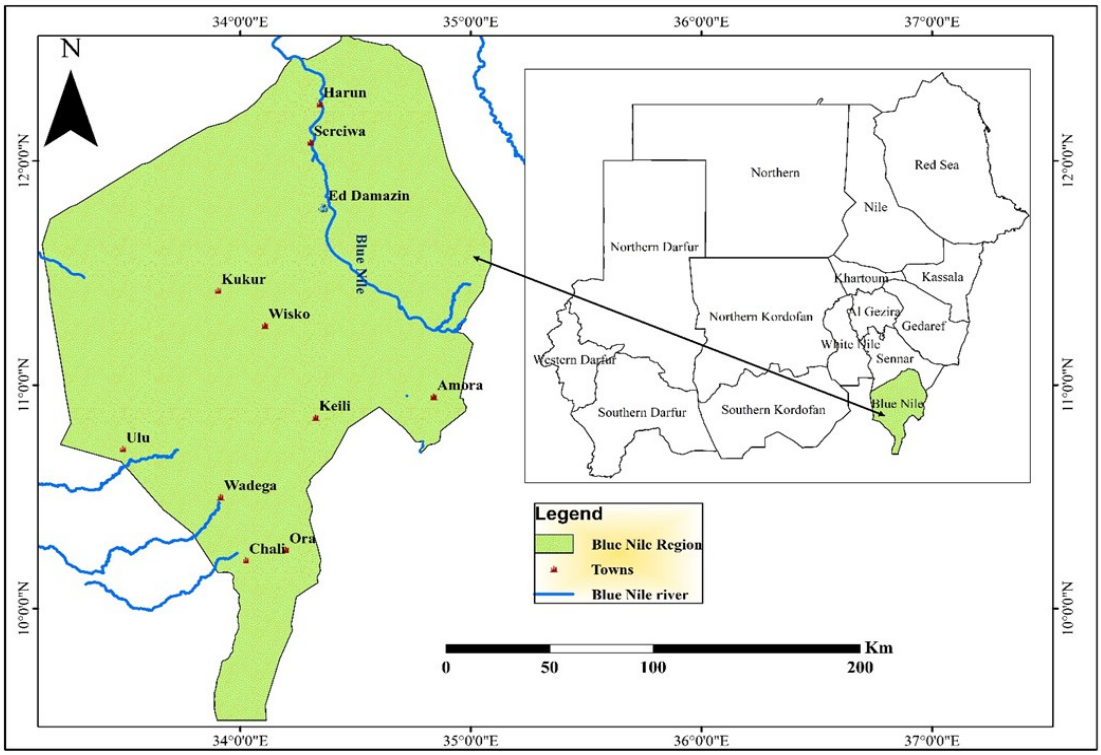

Fig. 1. *Showing the location map of the Blue Nile Region, situated in southeastern Sudan*

Table 1. Definition and calculation of some vegetation indices and Remote sensing equations

Vegetation Index	Abbreviation	Formula	Reference
Normalized Difference Vegetation Index (NDVI)	NDVI	$NDVI = \frac{(NIR - R)}{(NIR + R)}$	Hano *et al.* (2015)
Soil Adjusted and Atmospheric Resistant Vegetation Index	SARVI	$SARVI = \frac{NIR - RB_{(1+L)}}{NIR + RB + L}$ $RB = R - y(B - R)$	Hyvärinen *et al.* (2019)
Soil Adjusted Vegetation Index	SAVI	$SAVI = \frac{NIR - R_{(1+L)}}{NIR + R + L}$	Hyvärinen *et al.* (2019)
Vegetation Health Index	VHI	$\mathrm{VHI} = 0.5\mathrm{VCI} + 0.5\mathrm{TCI}$	Adam *et al.* (2023)
Bare Soil Index	BSI	$BSI = \frac{(SWIR2 + R) - (NIR + B)}{(SWIR2 + R) + (NIR + B)}$	Liu *et al*., (2022)
Topsoil Grain Size Index	TGSI	$TGSI = \frac{(R - B)}{(R + B + G)}$	Kumar *wt al.,* (2022)

NIR – near infrared wavelength, R-red wavelength, L- a value of 0.5 _ – a value of 1 G-green wavelength, B- blue wavelength, SWIR1 and SWIR2 shortwave infrared

(2014) characterized the area as part of the low-rainfall woodland savannah belt.The area is home to species such as Habil (*Combretum sp*), Talih (*Acacia seyal*), Sailack (*Anoguessis schematic*), *Ansora anise*, Naal, and Ankoj. These species thrive in the gently undulating landscape.

Methodology

The methodology involved several processes and approaches to achieve the research study's objectives. Remote sensing was utilized, and GIS employed various approaches, following several steps: (i) Careful selection of satellite imagery data based on temporal and spectral resolutions (Ejersa *et al*., 2021), (ii) Thorough image pre-processing and enhancement were tested to ensure the accuracy of research results. (iii) Following Hano (2013), the integration of biophysical indices and in situ data was used to evaluate soil degradation (vegetation and soil), including the Normalized Difference Vegetation Index (NDVI), Soil Adjusted Vegetation Index (SAVI), Soil Adjusted and Atmospheric Resistant Vegetation Index (SARVI), Vegetation Health Index (HVI), Topsoil Grain Size Index (TGSI), and Bare Soil Index (BSI), (iv) Correlation and modeling approach: the model was fitted and correlation of remote sensing (RS) data was calculated to identify relationships between different factors and analyze the reasons for land use pattern changes and land degradation (Wang *et al*., 2023).

Data selection and collection

Four cloud-free images from different sensors (TM Landsat 1993, ETM Landsat 2003, ASTER 2013, and OLI Landsat 2023) with 30m spatial resolution were selected. All were downloaded from the United States Geological Survey (USGS-GLOVIS) repository (https://earthexplorer.usgs.gov/). Field surveys were conducted during the dry season in May 2024 to collect and validate data about VIs and SIs. The movement and accumulation of sand, recognized as essential biophysical indicators of soil degradation, were assessed. Additionally, we evaluated the extent of forest degradation, characterized by sparse shrubs and trees. The accurate classification of soil types was achieved using the TGSI. Throughout the survey, a global positioning system (GPS) was extensively used to support our observations of both vegetation and soil (FAO, 2006; Soil Survey Staff, 2014).

Biophysical Indices Approach

A set of vegetation and soil indices derived from satellite imagery was utilized to identify soils affected by degradation. Table 1 shows the specifications of vegetation and soil indices. The combination of VI and SI was to enhance the accuracy of information for assessing land degradation in semiarid regions.

Data analysis

After conducting a ground survey and gathering information about the vegetation and soil conditions, various vegetation and soil indices (NDVI, SAVI, SARVI, EVI, HVI, TGSI, BSI, and NDSI) were computed using ArcGIS 10.8 software. Statistical parameters (Mean, Standard deviation, Maximum, and Minimum) were calculated based on the imagery data.

Image classification

The R^2, Kappa, and Principal Component Analysis (PCA) statistics were computed to quantify the strength of relationships between individual vegetation indices and land-use classes. These statistical parameters with values close to 1 signify a strong relationship, predict-

ing that a specific land-use type aids in identifying the most relevant vegetation indices for distinguishing among various land-use classes. To assess the classification methods' reliability, consistency, and computational efficiency, and to enhance accuracy. This integrated approach ensures a robust, interpretable, and accurate analysis of the relationships between vegetation and land use by creating a class hierarchy using fuzzy logic (Wang et al., 2023). The diagram illustrates the approach used for image classification (Fig. 2); the membership function fuzzy classification process.

Stepwise multiple parameters for land degradation analysis

The key land degradation indicators in the study area were identified, including vegetation and soil indices.

The response variables, such as the vegetation health index and topsoil grain size index rates, were defined alongside the predictor variables, which included NDSI, EVI, and NDVI.

Maps depicting both observed and predicted levels of degradation were developed to inform policy and management recommendations, quantifying the impact of each environmental covariate on degradation.

Kriging Modelling steps

Kriging is a geostatistical method used to interpolate and predict values at unsampled locations based on the spatial structure of the data.

Geospatial data was collected from known locations and values to identify soil status corresponding to the values of indices.

An experimental variogram was computed to quantify the spatial variability between data points based on their distance.

The fitted variogram was then utilized, and Kriging equations were applied to estimate values at unsampled locations.

Model performance

The correlation analysis, Kappa analysis, Principal Component Analysis (PCA), and Correlation metrics were used to assess the accuracy of the performance of the model (Table 3, Fig. 13). The Kriging model was validated by comparing predicted values with observed values at established locations. The spatial prediction maps were created to illustrate estimated values across the study area and evaluate the spatial patterns and uncertainties associated with these predictions.

RESULTS

Assessment of vegetation degradation using appropriate Vegetation Indices

The different VI and SI indices were tested and compared in the semiarid environment of Sudan.

The calculated vegetation indices values from Landsat 5, 7, 8, and 9 images (Fig. 3) over 30 years (A=1993, B=2023) indicated a noticeable decrease in NDVI values across different periods. The degradation indicators were observed in the photo location, which was taken in the study area.

Determination of land degradation

Based on the results in Fig. 3, the vegetation index was chosen to assess soil degradation in the study area. It effectively depicted the recent spatial distribution of degradation severity and highlighted the observed trends shown in Fig. 4.

Distribution of vegetation

The geospatial vegetation maps for 1993 to 2023 showed that dense and moderately dense vegetation cover is concentrated in vast parts of the area, while sparse vegetation is small and dispersed throughout the study area (map A). Therefore, in map B, the dense and moderately dense vegetation cover was near the Blue Nile River and small parts within the area, while sparse vegetation was more widely dispersed throughout the study area (Fig. 4).

In 1993, the vegetation cover index revealed that sparse areas accounted for about 9% of the total region, sparse and fallow land made up 11%, moderately dense vegetation covered 33%, and dense areas, representing agricultural and forestry zones, constituted the highest value at 41%. Water bodies covered 6% of the total area. By 2023, the distribution had shifted: sparse areas increased to 31%, sparse and fallow land to 20%, moderately dense areas decreased to 18%, dense areas to 21%, and water bodies expanded to 10% of the total area (Fig. 4).

Distribution of Vegetation Index

NDVI observations for the study area were compared across these periods. The results showed a significant downward trend in NDVI values in the study area, which represents the semiarid zones (Fig. 5). The A image displayed a high density of vegetation, while the D image exhibited a significant decrease in vegetation density, indicating a potentially severe impact of degradation in the area (Fig. 5).

The lower vegetation cover values mainly indicated bare land and rocky areas, while higher values corresponded to vegetation with higher moisture content. These values varied based on the density of plants in the region. In 1993, vegetation covered approximately 67% of the total area, as calculated by the NDVI (Fig. 5). By 2023, this percentage had declined to around 45%, marking a 22% decrease in vegetation cover over 30 years (Fig. 6). This indicates a continuous deterioration of vegetated surfaces up to the time of this study, suggesting a rapid decline in vegetation health.

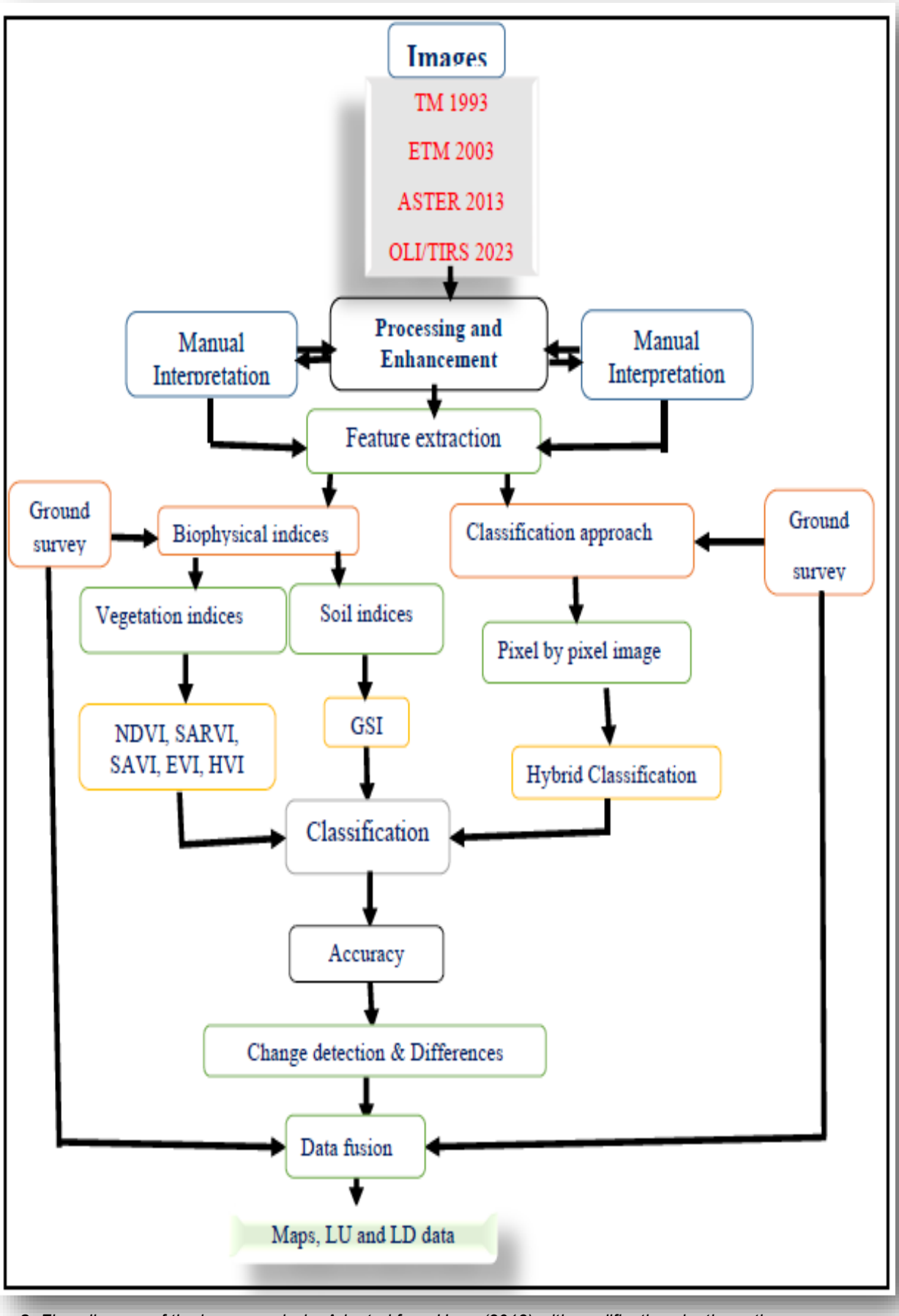

Fig. 2. *Flow diagram of the image analysis, Adapted from Hano (2013) with modifications by the author*

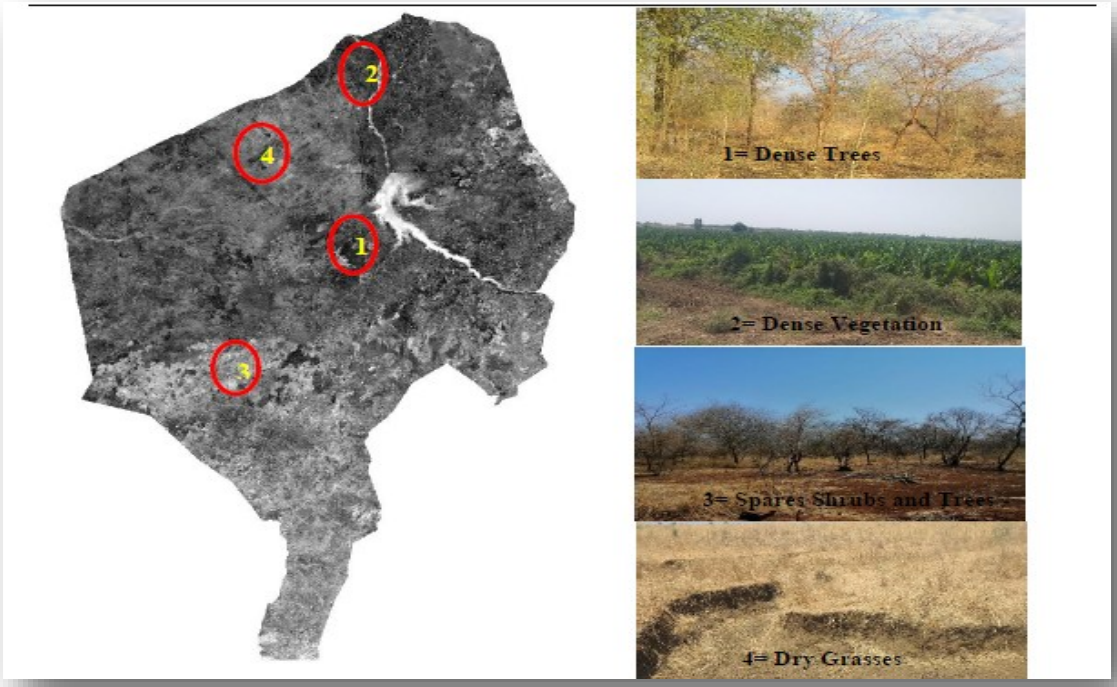

Fig. 3. *Temporal analysis comparing land degradation (1-4) from 1993 to 2023 with field observations in photos 1, 2, 3, and 4 in the Blue Nile Region*

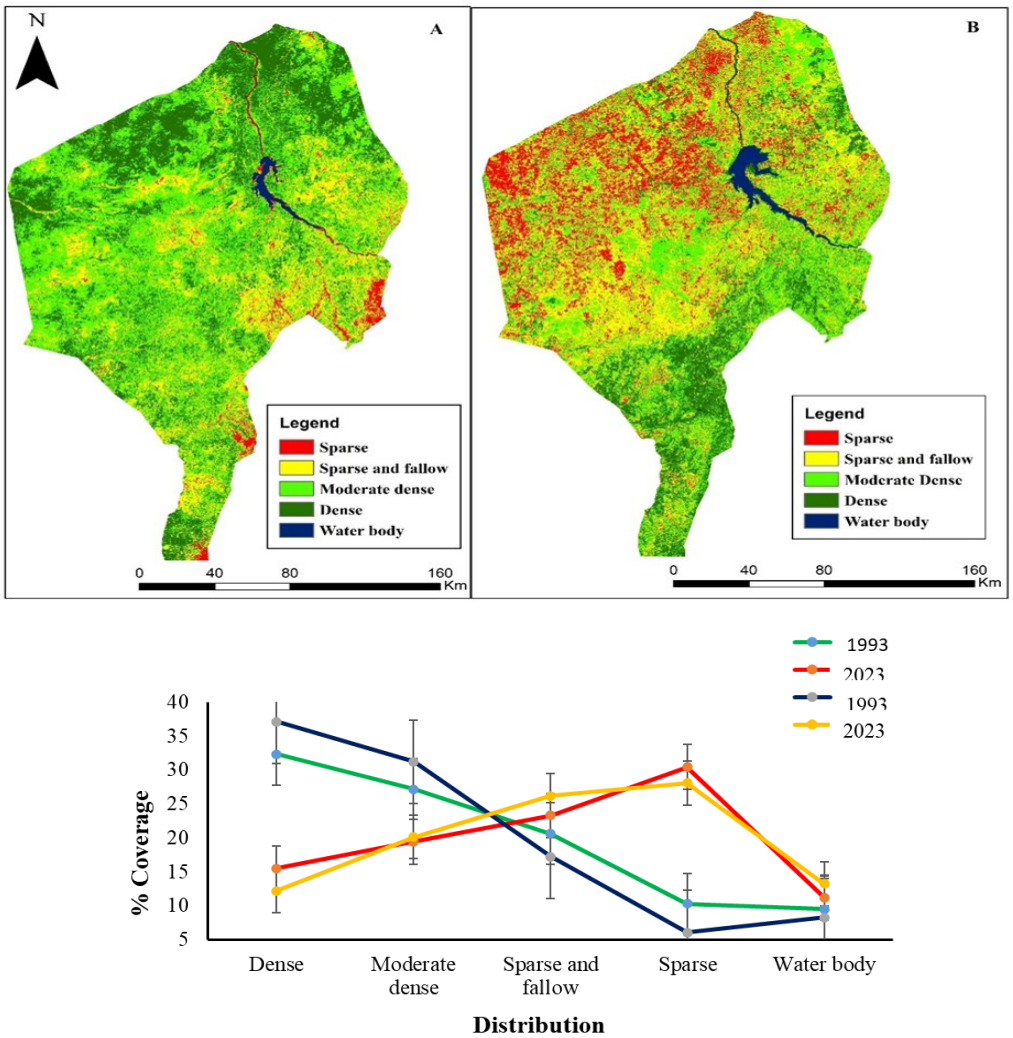

Fig. 4. *Spatial distribution of vegetation across the study area (1993 to 2023)*

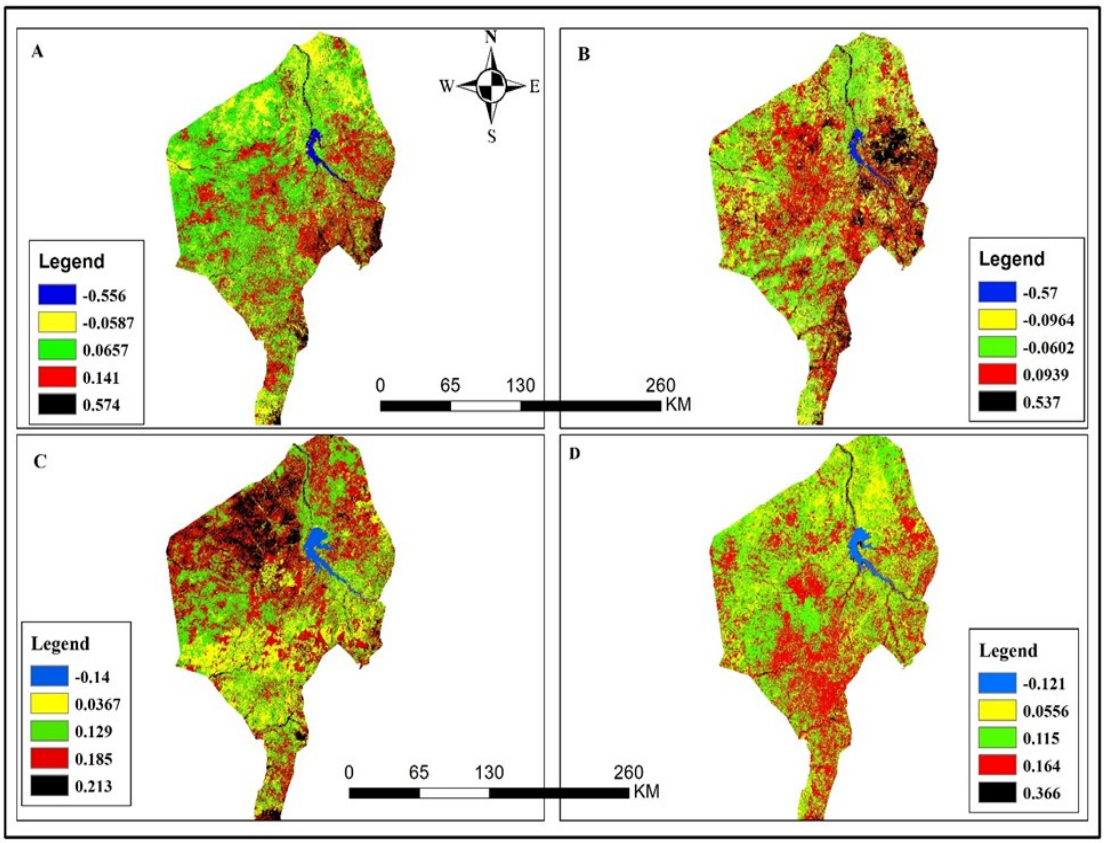

Fig. 5. *Distribution map of NDVI in Blue Nile Region (A=1993, B=2003, C=2013, D=2023)*

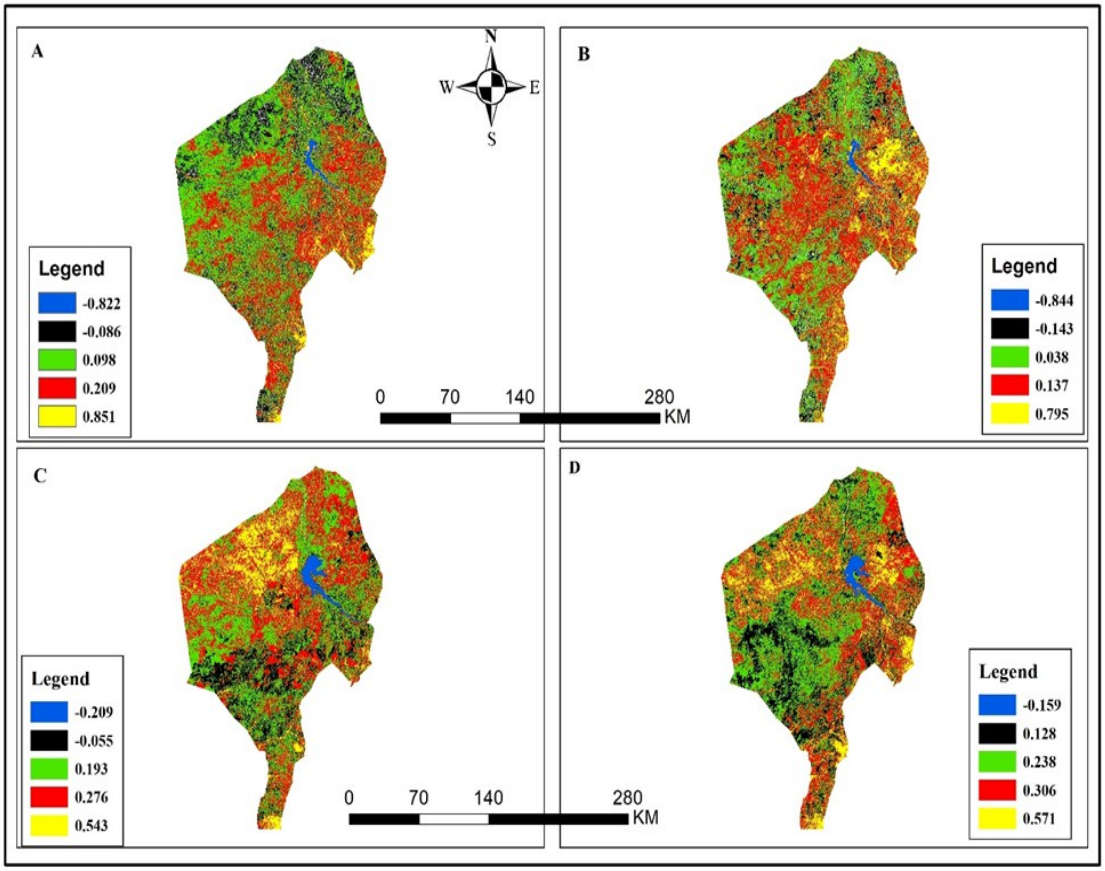

Fig. 6. *Distribution of the (SAVI) in the study area (A=1993, B=2003, C=2013, D=2023)*

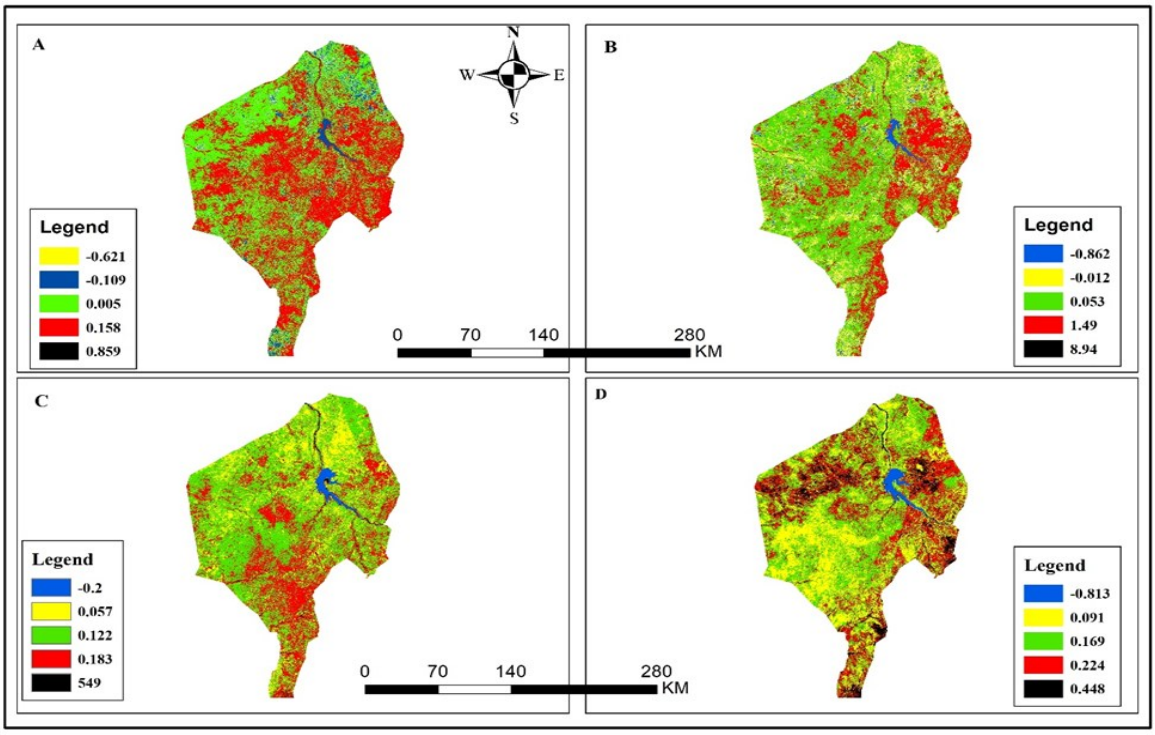

Fig. 7. *Distribution of Soil Adjusted and Atmospheric Resistant Vegetation Index (SARVI)*

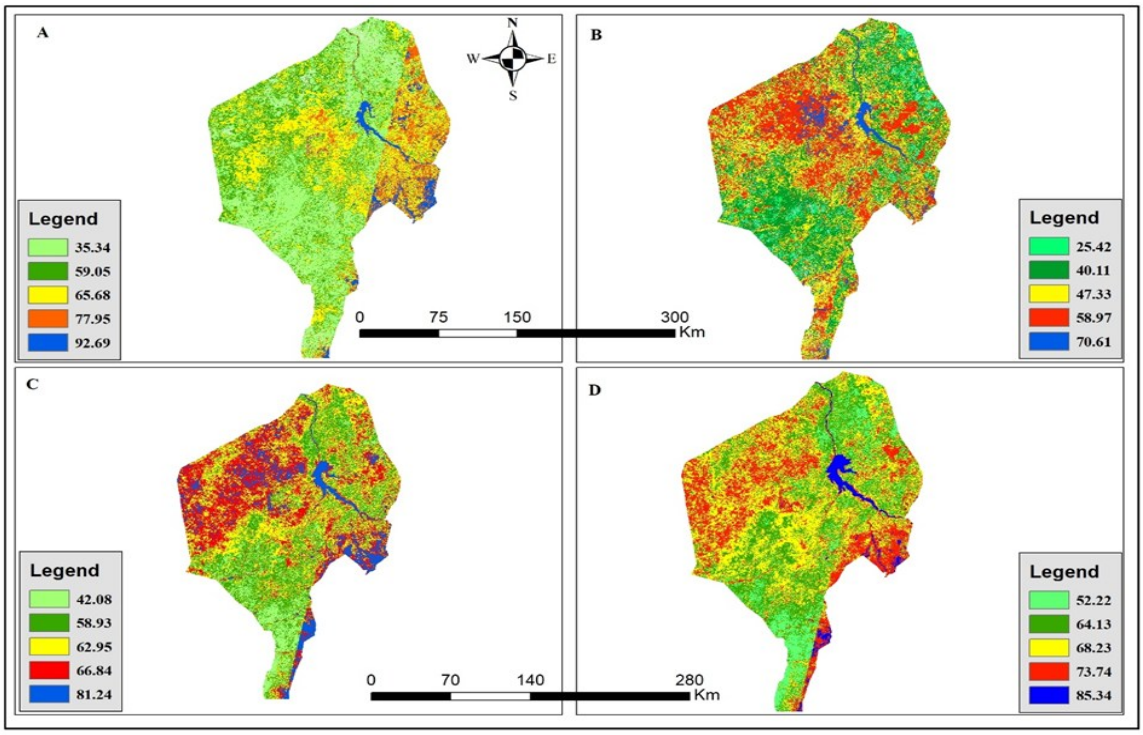

Fig. 8. *Distribution of VHI across study area (A=1993, B=2003, C=2013, D=2023)*

The Soil Adjusted Vegetation Index (SAVI) was analyzed by adjusting the reflection spectra in the NIR-red wavelength range to study the interaction between soil and vegetation through vegetative canopies (Fig. 6).

The results indicated that SAVI has a high sensitivity to soil background. It was observed that an optimal value for vegetation reflectance normalizes the soil effects and makes SAVI suitable across a range of vegetation densities, particularly in densely vegetated areas. In 1993, SAVI indicated that dense vegetation covered about 27,086.78 km² (71% of the total area), but by 2023, this had decreased to 15,641.66 km² (49%). The most significant variation among vegetation and soil surface characteristics was identified as the optimal value for surface coverage (Fig. 7).

An analysis of variance was used to adjust all available values within the coverage range using the Soil Adjusted and Atmospheric Resistant Vegetation Index (SARVI), which minimized soil influence on variables related to vegetated cover. In 1993, the SARVI index indicated high vegetation cover with dense vegetation distributed throughout the area around 73% (Fig 7). However, by 2023, the SARVI index revealed a significant reduction in vegetation density across the same region less than 38% (Fig 7). The VHI is acritical tool for identifying soil condition. It indicates that dense vegetation typically grows in fertile soil with sufficient nutrients and moisture, while sparse or fallow vegetation often indicates poor soil conditions, such as nutrient depletion or erosion (Fig 8). Monitoring vegetation can help detect early signs of land degradation. In an investigation aimed at creating an effective framework to enhance the soil health in northwestern Iran, Adam *et al*. (2023) highlighted a significant positive correlation between the Soil Health Index (SHI) and the Vegetation Health Index (VHI). The models developed in their study can be applied to large-scale assessments of soil health conditions, providing valuable support in monitoring and mitigating soil degradation in agricultural lands.

In 1993, the VHI indicated high healthy vegetation values within the area, with healthy vegetation covering around 81% of the total area. The vegetation cover decreased to 53% in 2023, indicating soil erosion and degradation.

The TGSI and BSI are essential tools for identifying soil surfaces, and monitoring these indices can help detect early signs of land degradation. The results from TGSI demonstrated a positive correlation with soil types through measurements of soil spectral reflectance (refer to Fig. 9). In 1993, over 90% of the surface soil was characterized by fine particle sizes, indicating a predominance of clay soils, with an increase in fine clay particles alongside a corresponding decrease in sand content. Conversely, the BSI analysis indicated that 89% of the total area was not subject to erosion. By 2023, the content of fine and coarse sand in the topsoil had increased in most locations. The proportion of fine particles on the surface decreased to 78%, reflecting a reduction in clay and silt content, along with an increase in the BSI rate to 43% of the total area. This shift signifies a coarser texture in both the topsoil and subsoil layers of the study area.

The relationships between the calculated vegetation indices, as presented in Table 2 and Fig. 10, have direct practical implications. They clearly show the connections that indicate land degradation in the study area. These indices are directly related to soil quality and ecosystem health. These results align with findings from Mariano et al. (2018) who confirmed the correlations emphasize specific indices that are particularly sensitive to environmental stressors, such as drought and soil erosion in Northeastern Brazil.

The average values of the soil and vegetation indices for the study periods 1993 to 2023 are presented in Table 2. The results show the following means and standard deviations: -NDVI, SAVI, SARVI, VHI, TGSI, AND BSI: (0.03-0.14, 0.05-0.21, 0.07- 0.17, 66.14-68.7, -0.136-0.008, and 301.1-4494.7; with a standard deviation of 0.4-0.17, 0.6-0.26, 0.53- 0.19, 19.2- 10.9, 0.05-0.5, and 7209.9-1593.9) respectively. These values correspond to different periods of analysis during the study.

In addition, Figure 10 shows that in 1993, extensive vegetation cover throughout the area. However, a noticeable decline in vegetation cover began in 2003 and persisted through 2013 and 2023. This gradual decrease ultimately resulted in the current degradation observed in the region. These patterns underscore the lasting impact of environmental factors, such as drought, on the health of vegetation and soil quality in the study area.

Spatial distribution of land cover and land degradation

Multiple stepwise parameters were utilized to develop models that describe the performance of kriging. The resulting predicted map classified land degradation into six categories: very severe degradation, severe degradation, moderate degradation, light degradation, no degradation, and water bodies (Fig. 11).

The degradation assessment in 1993 shows that the areas of very severe degradation had an overall low of 5.6%, severe degradation of 7.2%, moderate degradation of 13.8%, light degradation of 27.5%, no degradation of 35.4%, and water bodies of 10.5%. However, in 2023, the map showed a sharp and alarming rise in land degradation, with very severe degradation reaching 21.4%, severe degradation at 30.5%, moderate degradation at 16.3%, light degradation at 11.3%, no degradation at 8.3%, and water bodies at 12.2%, respectively. This comparison highlights the significant shift in land conditions over the past three decades, with the most recent data revealing the current state of the environment.

The analysis of land degradation levels, in conjunction with land use and land cover changes from 1993 to 2023, reveals notable trends that help explain the shifts in land conditions (Fig. 12). During this period, the interaction between human activities, land management practices, and environmental factors contributed significantly to the changes in land degradation. In 1993, the landscape consisted mostly of agricultural land, natural vegetation, and water bodies, with less urban development.

The assessment of this period showed that non-degraded land (35.4%) and lightly degraded areas (27.5%) made up the largest part of the landscape. These areas were mainly associated with agricultural land, grasslands, and natural vegetation, which experienced minimal human disturbance. Moderate degrada-

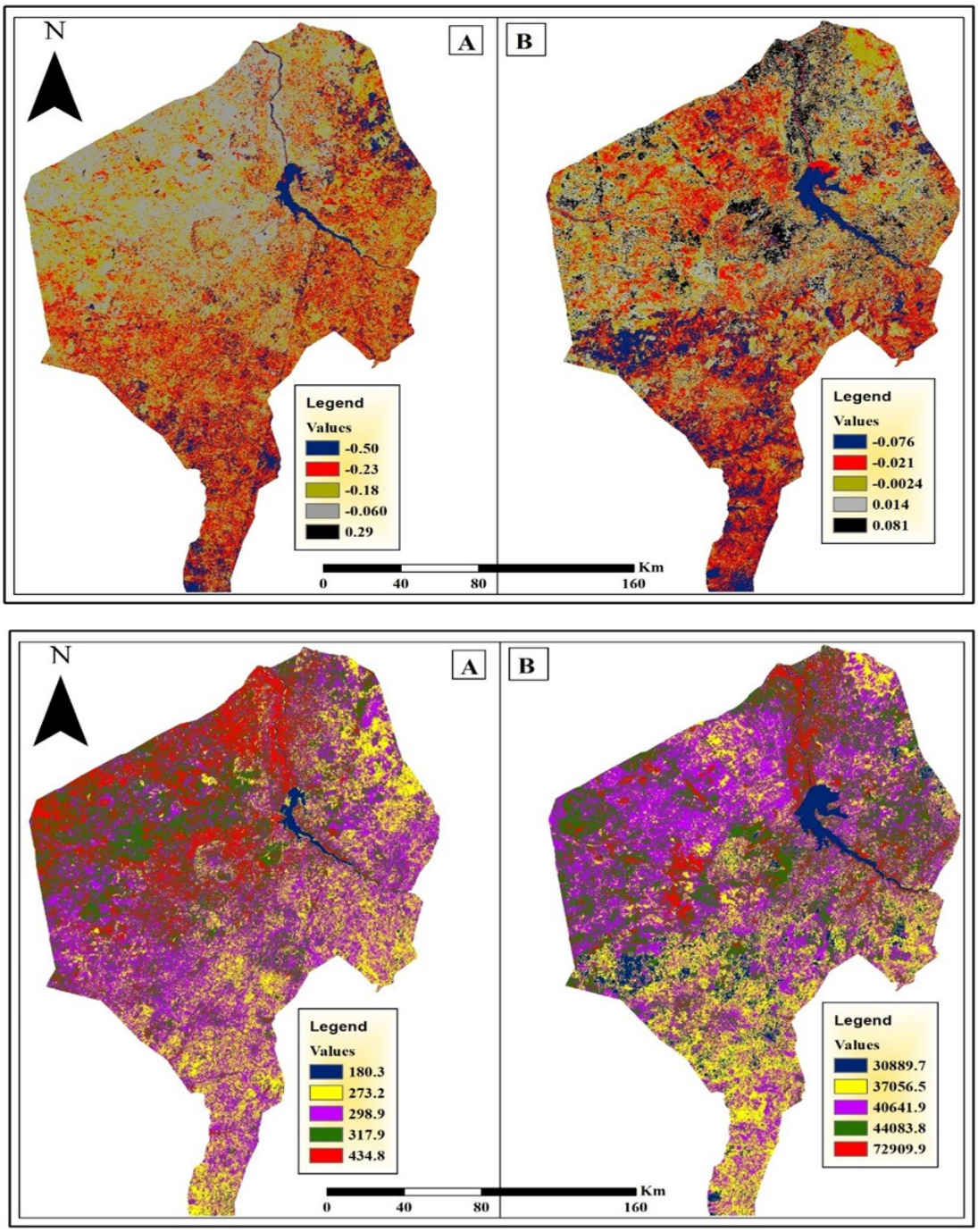

Fig. 9. *Temporal Variation in Topsoil Grain Size Index and Bare Soil Index (1993–2023) A= 1993, and B= 2023*

Table 2. Descriptive statistics of value indicators in the study area within different time periods

	1993				2023			
Variables	**Min**	**Max**	**Mean**	**Std.Dev**	**Min**	**Max**	**Mean**	**Std.Dev**
NDVI	-0.55	0.57	0.03	0.4	-0.1	0.38	0.14	0.17
SAVI	-0.82	0.85	0.05	0.6	-0.15	0.57	0.21	0.26
SARVI	-0.62	0.85	0.07	0.53	-0.08	0.44	0.17	0.19
VHI	35.34	92.69	66.14	19.2	52.22	85.34	68.7	10.9
TGSI	-0.5	0.29	-0.136	0.05	-0.076	0.081	-0.008	0.5
BSI	180.3	434.8	301.1	91.5	3089.7	7209.9	4494.7	1593.9

tion (13.8%) occurred in areas with more intensive agricultural activities and early signs of deforestation. Severe and very severe degradation accounted for 7.2% and 5.6% respectively. Water bodies represented 10.5% of the area, maintaining their integrity due to relatively stable environmental conditions. In 2023, significant changes in land use and land cover were observed. These changes were driven by increased urbanization, deforestation, and the expansion of agricultural land at the expense of natural ecosystems. As a result, degradation levels dramatically increased. Very severe degradation rose sharply to 21.4%, severe degradation increased to 30.5%, moderate degradation declined slightly to 16.3%, lightly degraded areas dropped to 11.3%, and non-degraded land decreased to 8.3%. These changes reflect the overall deterioration of land health and the encroachment of degraded areas into previously stable regions. Water bodies remained relatively stable, slightly increasing to 12.2%, likely due to shifts in hydrological patterns or land use planning around water resources.

Assessment of model performance

The degradation maps showed a strong relationship with vegetation indices such as NDVI, SARVI, SAVI, and EVI. These reliable maps indicated a significant relation with the mentioned vegetation indices.

Correlation analysis examined the relationship between soil and vegetation indices and soil degradation. Strong correlations were observed between specific vegetation indices (e.g., NDVI, SAVI) and degradation categories. The correlation coefficients (r = 0.52) indicated how well the indices predicted various levels of land degradation. Strong positive correlations were observed between soil and vegetation indices, such as TGSI, NDVI, and VHI, and the degradation categories representing soil health and vegetation stress. Conversely, strong negative correlations were observed between specific soil indices, such as the BSI, and vegetation indices, including NDVI and SAVI. A moderate correlation was also identified between TGSI and BSI, as shown in Table 3.

Kappa analysis assessed the agreement between the predicted soil degradation map and actual field observations. The overall Kappa value for the soil degradation map 1993 was 0.62, indicating substantial agreement between the predicted and observed degradation levels. In 2023, the Kappa value was 0.72, reflecting an even stronger agreement due to more detailed and accurate spatial data in the modelling process. This improvement in Kappa over time shows that the model has become more reliable in predicting soil degradation trends due to better data and enhanced modelling techniques.

Principal Component Analysis (PCA) was used to reduce the dimensionality of the vegetation indices while retaining the essential variables explaining variance in soil degradation patterns. The first principal component (PC1) explained around 55% of the variance and was strongly related to critical indicators of land health such as NDVI and EVI. The second principal component (PC2) explained 23% of the variance and was associated with variables indicating soil compaction and stress on vegetation. The first two PCs (PC1 PC2) captured about 78% of the total variability in the dataset, making them crucial in understanding the spatial degradation patterns. The PCA helped to simplify the model without losing critical information, thereby improving the model's interpretability and computational efficiency.

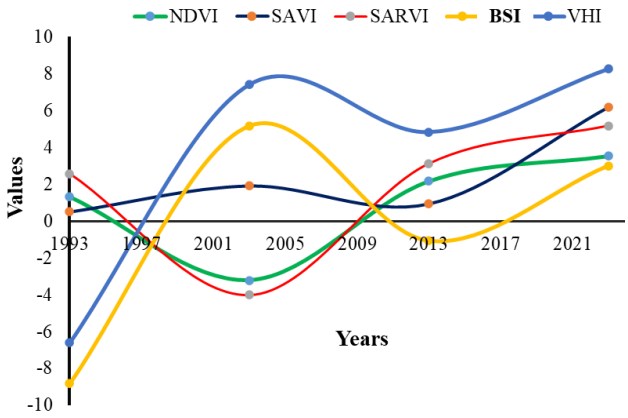

Fig. 10. *Distribution of vegetation indices during different periods of time*

DISCUSSION

The NDVI, SARVI, SAVI, VHI, TGSI, and BSI are commonly used to understand the connection between vegetation cover and soil degradation, which can be influenced by drought, land use, and climatic variations. As mentioned by Hano (2013), Nzuza et al. (2021), and Kumar et al. (2022) on their research on SIs and VIs was used to assess land degradation. The resulting map in present study showed that severe LD was dominant and widely distributed in the northern and central parts of the area, attributed to the presence of sparse herbaceous plants, grasses, and scattered shrubs growing on fragile bare soil (Fig. 3). This is attributed to soil degradation and changes in soil surface characteristics due to the high rate of drought and low soil capability, which result from the impact of agricultural practices on land use and soil suitability (Fig. 4). Numerous studies have documented that arid and semiarid zones are highly susceptible to degradation due to drought and climate change effects (Ayoub, 1998; Vicente-Serrano *et al*., 2015; Abdelhak, 2022; Shao *et al*., 2024) who researched and mapped LD across Sudan, world semi arid zones, and northwest of China. The drought significantly impacts vegetation types, soil nutrient dynamics, and spatial distribution. Additionally, topography affects soil degradation through erosion. (Gray *et al*., 2015; Wiesmeier *et al*., 2019) in eastern

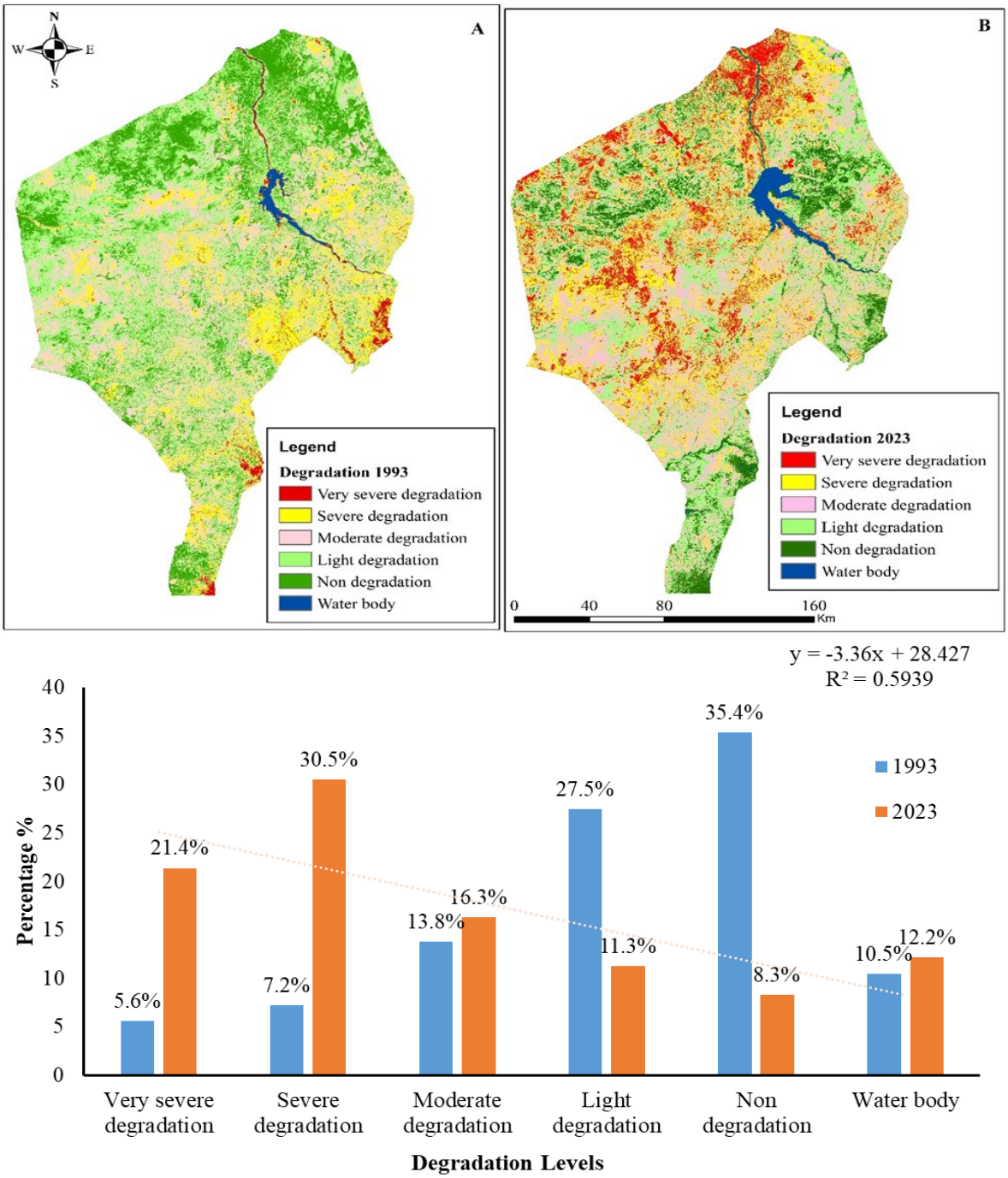

Fig. 11. *Spatial distribution of land covers and land degradation (1993 to 2023)*

Table 3. Descriptive Statistics and Correlation Matrix of Soil and Vegetation Indices

Variables	Means	Std.Dev	TGSI	BSI	NDVI	SAVI	SARVI	VHI
TGSI	-0.07	0.17	1.00					
BSI	2397.89	840.54	0.76	1.00				
NDVI	0.07	0.29	0.99	-0.92	1.00			
SAVI	0.15	0.44	0.68	-0.89	0.99	1.00		
SARVI	0.04	0.49	0.77	0.88	0.99	0.79	1.00	
VHI	67.44	16.81	0.98	0.90	0.89	0.99	-0.98	1.00

Table 4. PCA to extract the key land degradation indicators in the study area

	PC		
Index	Factor1	Factor2	Factor3
NDVI	0.243379	-0.232018*	-0.081084
SAVI	-0.77857	-0.502572	0.084828
SARVI	0.49101**	-0.309577	0.188812
EVI	0.38033	0.891199	0.096254
HVI	0.4143*	0.89247	-0.277317
LU/LC	0.55267**	-0.014938	0.82996*
Total %	0.341537	0.277042	0.141907
Eigenvalue	8.194872	3.924002	2.550491
Weighing	0.463012	0.221707	0.144103
Land Degradation	78%		

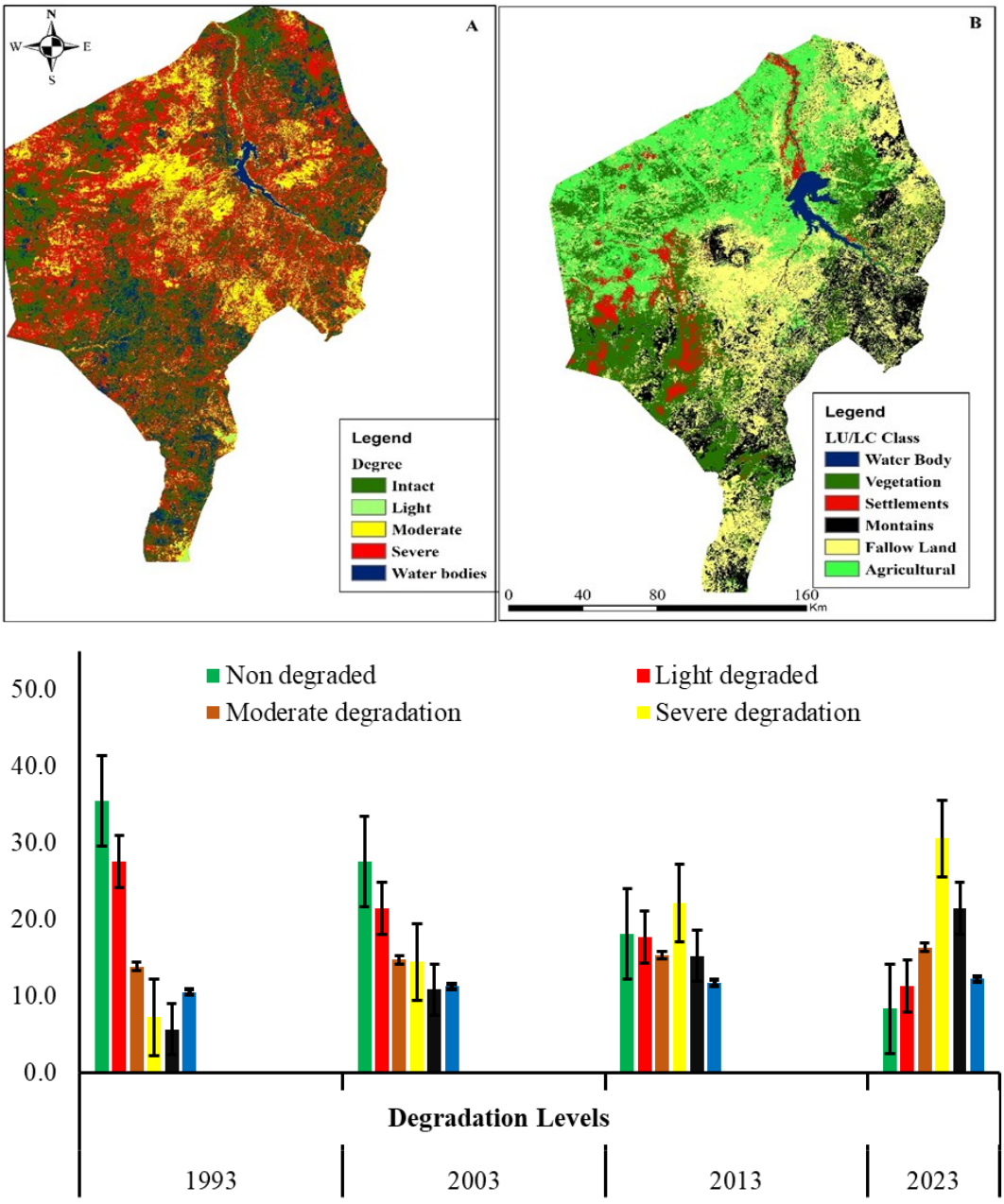

Fig. 12. *Spatial distribution of land degradation categories in the study area*

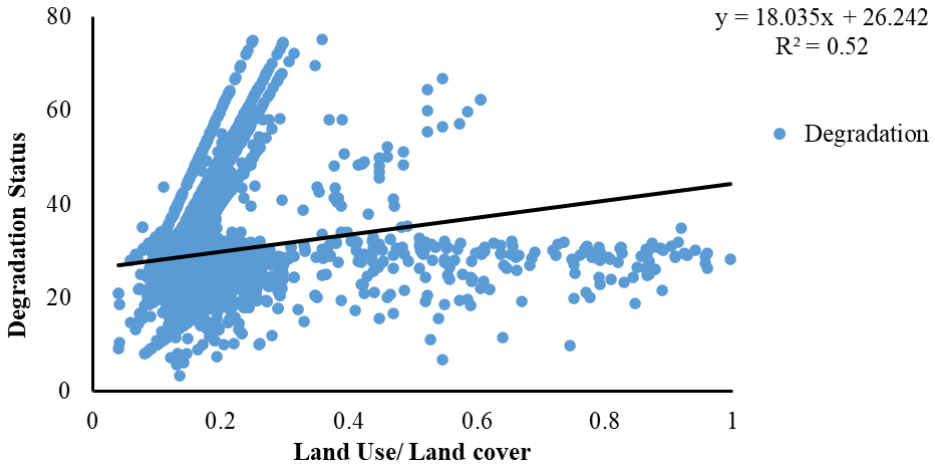

Fig. 13. *Distribution correlation analysis for land use and degradation in the study area*

Australia.

A significant decline in NDVI during the study was correlated with reduced vegetation cover and soil degradation (Fig. 5). The studies conducted by many researchers (Dutta *et al*., 2013; Wang *et al*., 2023; Otieno *et al*., 2025) on Eastern Rajasthan of India and Kenya have proven that predicting the decrease in NDVI values and annual variation of global drought, coupled with vegetation and climate change variability, can indicate land degradation. The variations in SAVI and SARVI (Figures 6, 7) indicate the degree of soil influence on low vegetation cover, helping to confirm the role of soil degradation due to poor vegetation and highlighting how environmental conditions contributed to soil degradation during drought seasons. Kumar *et al*. (2022), Aji et al. (2021), and Yengoh et al. (2015) highlighted the significant relationship between NDVI and SAVI in determining soil degradation. According to Yasin *et al.* (2025) focusing on Sudan, the SARVI, is valuable in determining the extent to which deforestation and natural vegetation are degraded. The different study periods showed that high VHI values in 1993 indicated healthy vegetation, while low VHI values confirmed vegetation stress due to drought, leading to soil degradation (Fig. 8). The results align with findings from (Desta., et al. 2021; and Beyene et al. 2023) focus on Ethiopia, the health of vegetation cover reflects the health of the soil and its ability to resist degradation.

The TGSI demonstrated a steady increase from 2013 to 2023, with an average annual growth rate of 3.5%. This upward trend may be linked to extended periods of reduced rainfall, which result in soil compaction and the erosion of finer particles. In contrast, the BSI displayed significant inter-annual variability, with peak values occurring during dry seasons (Fig. 9). This fluctuation suggests that seasonal factors play a role, as decreased vegetation cover exposes bare soil. These patterns are consistent with the study's findings by Liu *et al*. (2022) on China, while Halászová *et al*. (2024) conducted their research in the south-western part of Slovakia. Both regions experience similar land degradation pressures that influence soil indices, supporting the observed seasonal fluctuations in vegetation cover and soil exposure discussed in our study area (Blue Nile Region).

The findings indicated that NDVI and SARVI were more suitable for VI than SAVI and VHI for assessing the LD (Fig. 10) based on the vegetation degradation indicator in the semiarid zone. The produced map showed that the vegetation cover corresponded somewhat to the actual conditions in the study area. This is consistent with the findings of Hano *et al*. (2013), Wang *et al*. (2023), and Viet *et al*. (2024), who studied LD assessment by different indices in Sudan and Dak Nong, Vietnam.

The present study found a strong positive correlation between the spatial distribution of land covers and land degradation value with vegetation indices (r = 0.59, Fig. 11). Areas with low degradation values mainly represented healthy land with densely vegetated areas. The findings were consistent with those of de Oliveira *et al*. (2022), whose studies mapped land degradation in Ethiopia and showed that degradation trends increased from northeast to southwest (Savannah agro-ecological zone), corresponding to increasing vegetation density in the southwest part of our study area. The observed variations in degradation categories during different periods suggest that seasonal and climatic factors, such as droughts, strongly influence vegetation cover (Fig. 12). During drought periods, soil exposure to degradation and erosion increases, and organic matter levels decrease. Therefore, the spatial distribution of land degradation categories and land use change values showed a strong positive correlation (r = 52, Fig. 13). Strong positive correlations between the (TGSI, NDVI, VHI) indicate that these indices work complementarily in assessing soil degradation. In contrast, strong negative correlations between the (BSI, NDVI, SAVI) suggest that higher soil degradation indices are associated with poorer vegetation health. This high-

lights the relationship between soil exposure and erosion. Additionally, the moderate correlation between TGSI and BSI reflects their role in evaluating surface soil conditions (Table 3). Similar patterns were observed in studies by Raiesi *et al*. (2020), Fadl *et al*. (2024), and Khusfi *et al*. (2020), which noted significant variations in the correlations between soil and vegetation indices in arid regions (Central Iran, Egypt, and Markazi Province, Iran) when assessing land degradation. The Kappa value shows high accuracy in land use patterns and degradation. Moreover, the principal component of the land degradation categories showed a positive correlation with NDVI, SARVI, and land use change by a value of 78% (Table 4). Areas where vegetation indices decreased significantly over time corresponded with overgrazing, deforestation, and agricultural expansion areas, all of which contributed to soil degradation. Studies on the prediction of land degradation confirmed that assessing the model is essential. The studies conducted by de Oliveira *et al*. (2022) focus on Northeastern Brazil, whereas Orimoloye *et al*. (2022) carried out their research in South Africa. They emphasized the importance of verifying degradation models through statistical tests such as R, the Kappa coefficient, and RMSE. The results from these tests included an R^2 value of 0.43, a Kappa of 67%, and an RMSE of 1.33. These findings support the model accuracy assessment values used in the study of the Blue Nile region. Regression-based algorithms, principal components, correlation, and kappa analysis are very accurate methods to validate the model related to land degradation studies using remote sensing and modeling.

Conclusion

The study investigated the spatial distribution of land degradation in the Blue Nile Region, Sudan. It was observed that land degradation exhibited decreasing trends over different periods. The study found that NDVI, SARVI were slightly more effective than SAVI and VHI in assessing vegetation degradation in semiarid areas within the Blue Nile region. These indicators proved to be highly efficient in determining different types of soil degradation, thus aiding in the assessment of land degradation. Changes in land use patterns were also found to impact soil degradation, leading to degraded vegetation from 1993 to 2023. The study incorporated a fusion of remote sensing data to establish correlations and valid models of the impact of land use classes on land degradation in the semiarid zone at the spatiotemporal scale. This was achieved through statistical analyses, including Kappa analysis, correlation, and principal component analysis. The results indicated a medium-strong correlation between land degradation and vegetation indices related to land use patterns, suggesting that these factors contribute to land degradation. The generated land degradation maps were accurate and could provide quantitative estimations of degradation categories at a relatively low cost, thus serving as a valuable tool for environmental evaluation. However, it was noted that the produced land degradation map is relatively acceptable but could benefit from additional legacy data and environmental covariates to enhance its accuracy. Based on the findings of the study, it is recommended that (i) the Kriging models and correlation be utilized for predicting soil degradation via vegetation due to their relatively high accuracy and low cost, and (ii) more environmental covariates are required to improve the accuracy of the predicted land degradation map resulting from drought.

ACKNOWLEDGMENTS

The authors express their gratitude to the Pan Africa University, Life and Earth Sciences Institute (Including Health and Agriculture) - PAULESI, University of Ibadan, Ibadan, Nigeria, for their pivotal role in providing the Ph.D. scholarship opportunity and supporting this research. We also acknowledge the significant contribution of the Land and Water Research Centre (LWRC), Agricultural Research Corporation (ARC), and Land Evaluation Division, Wad Madani, Sudan, for providing the legacy soil profile database for the study area, which was instrumental in the success of this research.

Conflict of interest

The authors declare that they have no conflict of interest.

REFERENCES

1. Abdelhak, M. (2022). Soil improvement in arid and semiarid regions for sustainable development. In *Natural resources conservation and advances for sustainability* (pp. 73-90). Elsevier. doi.org/10.1016/B978-0-12-822976-7.00026-0.
2. Adam, K. K., Rezapour, S., Asadzadeh, F., & Nouri, A. (2023). An integrated approach for estimating soil health: Incorporating digital elevation models and remote sensing of vegetation. *Computers and Electronics in Agriculture*, *210*, 107922. doi.org/10.1016/j.compag.2023.107922.
3. Aji, A., Iryanthony, S. B., Sidiq, W. A. B. N., & Trihatmoko, E. (2021). Relationship between NDVI and the microbial content of soil in detecting fertility level at Semarang regency, Jawa Tengah Indonesia. *Nature Environment and Pollution Technology*, *20*(1), 425-432.
4. Ali, H., Etang, A., Fuje, H., & Touray, S. (2020). *Agricultural productivity and poverty in Rural Sudan.* World Bank.
5. Alredaisy, S. M. A. H. (2023). Reviewing indicators of climate change and their environmental impacts in Sudan. *International Journal of Recent Research in Interdisciplinary Sciences*, *10*(4), 7-16.
6. Ayoub, A. T. (1998). Extent, severity and causative factors of land degradation in the Sudan. *Journal of arid environments*, *38*(3), 397-409. doi.org/10.1006/jare.1997.0346.

7. Beyene, S., Regassa, A., Mishra, B. B., & Haile, M. (Eds.). (2023). *The soils of Ethiopia*. Berlin: Springer. doi.org/10.1016/j.iswcr.2021.04.008.
8. Chasek, P., Akhtar-Schuster, M., Orr, B. J., Luise, A., Ratsimba, H. R., & Safriel, U. (2019). Land degradation neutrality: The science-policy interface from the UNCCD to national implementation. *Environmental Science & Policy*, *92*, 182-190. doi.org/10.1016/j.envsci.2018.11.017.
9. de Oliveira, M. L., Dos Santos, C. A., de Oliveira, G., Silva, M. T., da Silva, B. B., de BL Cunha, J. E., & Santos, C. A. (2022). Remote sensing-based assessment of land degradation and drought impacts over terrestrial ecosystems in Northeastern Brazil. *Science of The Total Environment*, *835*, 155490. doi.org/10.1016/j.scitotenv.2022.155490.
10. Desta, G., Tamene, L., Abera, W., Amede, T., & Whitbread, A. (2021). Effects of land management practices and land cover types on soil loss and crop productivity in Ethiopia: A review. *International Soil and Water Conservation Research*, *9*(4), 544-554. doi.org/10.1016/j.iswcr.2021.04.008.
11. Dieng, M., Mbow, C., Skole, D. L., & Ba, B. (2023). Sustainable land management policy to address land degradation: linking old forest management practices in Senegal with new REDD+ requirements. *Frontiers in Environmental Science*, *11*, 1088726. doi.org/10.3389/fenvs.2023.1088726.
12. Dutta, D., Kundu, A., & Patel, N. R. (2013). Predicting agricultural drought in eastern Rajasthan of India using NDVI and standardized precipitation index. *Geocarto International*, *28*(3), 192-209. doi.org/10.1080/10106049.2012.679975
13.
14. Ejersa, M. T. (2021). Causes of land degradation and its impacts on agricultural productivity: A review. *International Journal of Research and Innovations in Earth Science*, *8* (3), 67-73.
15. Ekka, P., Patra, S., Upreti, M., Kumar, G., Kumar, A., & Saikia, P. (2023). Land Degradation and its impacts on Biodiversity and Ecosystem services. *Land and Environmental Management through Forestry*, 77-101. doi.org/10.1002/9781119910527.ch4.
16. Elnashi, R., & Ahamed, D. (2014). Characterization and Classification of Soils in the Blue Nile Basin Forests: Case Studies of Lembwa and El-Gazair Forest Reserves, Sennar State, Sudan.
17. Elzien, S. M., Sayed, E. K., Al-Imam, O. A., Hamed, H. B., Altigani, M. A., & Kheiralla, K. M. (2017). Genesis of Soils from Mafic and Ultramafic Rocks in Southeast Ingassana Hills Complex, Blue Nile State, Sudan.
18. Fadl, M. E., AbdelRahman, M. A., El-Desoky, A. I., & Sayed, Y. A. (2024). Assessing soil productivity potential in arid region using remote sensing vegetation indices. *Journal of Arid Environments*, *222*, 105166. doi.org/10.1016/j.jaridenv.2024.105166.
19. FAO (2006). Guidelines for soil profile description. (fourth edition), Rome, Italy
20. Gray, J. M., Bishop, T. F., & Wilson, B. R. (2015). Factors controlling soil organic carbon stocks with depth in eastern Australia. *Soil Science Society of America Journal*, *79*(6), 1741-1751. doi.org/10.2136/sssaj2015.06.0224.
21. Grillakis, M. G. (2019). Increase in severe and extreme soil moisture droughts for Europe under climate change. *Science of the Total Environment*, *660*, 1245-1255. doi.org/10.1016/j.scitotenv.2019.01.001.
22. Halászová, K., Lackóová, L., & Panagopoulos, T. (2024). Long-term evaluation of surface topographic and topsoil grain composition changes in an agricultural landscape. *Frontiers in Environmental Science*, *12*, 1445068. doi.org/10.3389/fenvs.2024.1445068.
23. Hano, A. I. A. (2013). Assessment of Impacts of Changes in Land Use Patterns on Land Degradation/Desertification in the Semiarid Zone of White Nile State, Sudan, by Means of Remote Sensing and GIS.
24. Hano, A. I. A. (2013). Assessment of impacts of changes in land use patterns on land degradation/desertification in the semiarid zone of White Nile State, Sudan, by means of remote sensing and GIS.
25. Hermans, K., & McLeman, R. (2021). Climate change, drought, land degradation and migration: exploring the linkages. *Current opinion in environmental sustainability*, *50*, 236-244. doi.org/10.1016/j.cosust.2021.04.013.
26. Hyvärinen, O., Timm Hoffman, M., & Reynolds, C. (2019). Vegetation dynamics in the face of a major land-use change: a 30-year case study from semiarid South Africa. *African Journal of Range & Forage Science*, *36*(3), 141-150. doi.org/10.2989/10220119.2019.1627582
27. Kabesh, M. L., & Afia, M. S. (1961). *Manganese ore deposits of the Sudan* (No. 9). Ministry of Mineral Resources, Geological Survey Department.
28. Khusfi, Z. E., & Zarei, M. (2020). Relationships between meteorological drought and vegetation degradation using satellite and climatic data in a semiarid environment in Markazi Province, Iran. *Iran. J. Rangel. Sci*, *10*, 204-216.
29. Kumar, B. P., Babu, K. R., Rajasekhar, M., & Ramachandra, M. (2022). Assessment of the visual disaster of land degradation and desertification using TGSI, SAVI, and NDVI techniques. In *Geospatial Modeling for Environmental Management* (pp. 261-279). CRC Press.
30. Liu, Y., Meng, Q., Zhang, L., & Wu, C. (2022). NDBSI: A normalized difference bare soil index for remote sensing to improve bare soil mapping accuracy in urban and rural areas. *Catena*, *214*, 106265. doi.org/10.1016/j.catena.2022.106265.
31. Mariano, D. A., dos Santos, C. A., Wardlow, B. D., Anderson, M. C., Schiltmeyer, A. V., Tadesse, T., & Svoboda, M. D. (2018). Use of remote sensing indicators to assess effects of drought and human-induced land degradation on ecosystem health in Northeastern Brazil. *Remote Sensing of Environment*, *213*, 129-143. doi.org/10.1016/j.rse.2018.04.048.
32. Merabti, A., Darouich, H., Paredes, P., Meddi, M., & Pereira, L. S. (2023). Assessing spatial variability and trends of droughts in Eastern Algeria Using SPI, RDI, PDSI, and MedPDSI—A novel drought index using the FAO56 evapotranspiration method. *Water*, *15*(4), 626. doi.org/10.3390/w15040626.
33. Minelli, S., Erlewein, A., & Castillo, V. (2017). Land degradation neutrality and the UNCCD: from political vision to measurable targets. *International Yearbook of Soil Law and Policy 2016*, 85-104. doi.org/10.1007/978-3-319-42508-5_9.
34. Mohamed, S. (2022). *Assessing Vulnerability and the Potential for Ecosystem-based Adaptation (EbA) in Sudan's Blue Nile Basin* (Master's thesis, The Ohio State University).
35. Naumann, G., Alfieri, L., Wyser, K., Mentaschi, L., Betts, R. A., Carrao, H., ... & Feyen, L. (2018). Global changes

in drought conditions under different levels of warming. *Geophysical Research Letters*, *45*(7), 3285-3296. doi.org/10.1002/2017GL076521.

36. Nzuza, P., Ramoelo, A., Odindi, J., Kahinda, J. M., & Madonsela, S. (2021). Predicting land degradation using Sentinel-2 and environmental variables in the Lepellane catchment of the Greater Sekhukhune District, South Africa. *Physics and Chemistry of the Earth, Parts A/B/C*, *124*, 102931. doi.org/10.1016/j.pce.2020.102931.
37. Orimoloye, I. R., Olusola, A. O., Belle, J. A., Pande, C. B., & Ololade, O. O. (2022). Drought disaster monitoring and land use dynamics: identification of drought drivers using regression-based algorithms. *Natural Hazards*, *112*(2), 1085-1106. Link.springer.com/article/10.1007/s11-69-022-05219-9
38. Otieno, T. A., Otieno, L. A., Rotich, B., Löhr, K., & Kipkulei, H. K. (2025). Modeling climate change impacts and predicting future vulnerability in the Mount Kenya forest ecosystem using remote sensing and machine learning. *Environmental Monitoring and Assessment*, *197*(6), 631. link.springer.com/article/10.1007/s10661-025-14089-0
39. Raiesi, F., & Salek□Gilani, S. (2020). Development of a soil quality index for characterizing effects of land□use changes on degradation and ecological restoration of rangeland soils in a semiarid ecosystem. *Land Degradation & Development*, *31*(12), 1533-1544. doi.org/10.1002/ldr.3553.
40. Shao, W., Zhang, Z., Guan, Q., Yan, Y., & Zhang, J. (2024). Comprehensive assessment of land degradation in the arid and semiarid area based on the optimal land degradation index model. *Catena*, *234*, 107563. doi.org/10.1016/j.catena.2023.107563.
41. Soil Survey Staff (2014). Keys to Soil Taxonomy, 12 editions. United States Department of Agriculture, Natural Resources Conservation Service, Washington, DC.
42. Taye, M. T., Willems, P., & Block, P. (2015). Implications of climate change on hydrological extremes in the Blue Nile basin: a review. *Journal of Hydrology: Regional Studies*, *4*, 280-293. doi.org/10.1016/j.ejrh.2015.07.001.
43. UNCCD. 2012. ZERO NET LAND DEGRADATION, A Sustainable Development Goal for Rio + 20 (PP.4-6).
44. Vicente-Serrano, S. M., Cabello, D., Tomás-Burguera, M., Martín-Hernández, N., Beguería, S., Azorin-Molina, C., & El Kenawy, A. (2015). Drought variability and land degradation in semiarid regions: Assessment using remote sensing data and drought indices (1982–2011). *Remote Sensing*, *7*(4), 4391-4423. doi.org/10.3390/rs70404391.
45. Viet, L. V., & Thuy, T. T. T. (2024). Drought sensitivity analysis of meteorological and vegetation indices in Dak Nong, Vietnam. *Journal of Water and Climate Change*, jwc2024661. doi.org/10.2166/wcc.2024.661.
46. Wang, J., Zhen, J., Hu, W., Chen, S., Lizaga, I., Zeraatpisheh, M., & Yang, X. (2023). Remote sensing of soil degradation: Progress and perspective. *International Soil and Water Conservation Research*, *11*(3), 429-454. doi.org/10.1016/j.iswcr.2023.03.002.
47. Webb, N. P., Marshall, N. A., Stringer, L. C., Reed, M. S., Chappell, A., & Herrick, J. E. (2017). Land degradation and climate change: building climate resilience in agriculture. *Frontiers in Ecology and the Environment*, *15*(8), 450-459. doi.org/10.1002/fee.1530.
48. Wiesmeier, M., Urbanski, L., Hobley, E., Lang, B., von Lützow, M., Marin-Spiotta, E., ... & Kögel-Knabner, I. (2019). Soil organic carbon storage as a key function of soils-A review of drivers and indicators at various scales. *Geoderma*, *333*, 149-162. doi.org/10.1016/j.geoderma.2018.07.026.
49. Yadeta, D., Kebede, A., & Tessema, N. (2020). Climate change posed agricultural drought and potential of rainy season for effective agricultural water management, Kesem sub-basin, Awash Basin, Ethiopia. *Theoretical and Applied Climatology*, *140*, 653-666. doi.org/10.1007/s00704-020-03113-7
50. Yasin, E. H., Siddig, A. A., Diab, E. E., & Czimber, K. (2025). Evaluating the Efficiency of Two Ecological Indices in Monitoring Forest Degradation in the Drylands of Sudan. *Remote Sensing*, *17*(13), 2298. doi.org/10.3390/rs17132298.
51. Yengoh, G. T., Dent, D., Olsson, L., Tengberg, A. E., & Tucker III, C. J. (2015). *Use of the Normalized Difference Vegetation Index (NDVI) to assess Land degradation at multiple scales: current status, future trends, and practical considerations*. Springer.
52. Zhang, Q., Shao, M., Jia, X., & Wei, X. (2019). Changes in soil physical and chemical properties after short drought stress in semi-humid forests. *Geoderma*, *338*, 170-177. 10.1016/j.geoderma.2018.11.051.doi.org/10.1016/j.geoderma.2018.11.051.